



OPEN

Solid-phase synthesis and pathological evaluation of pyroglutamate amyloid- β_{3-42} peptide

Illhwan Cho^{1,2}, HeeYang Lee^{1,2}, Donghee Lee^{1,2}, In Wook Park^{1,2}, Soljee Yoon^{1,2,3}, Hye Yun Kim^{1,2} & YoungSoo Kim^{1,2,3,4}

Pyroglutamate amyloid- β_{3-42} ($A\beta_{pE3-42}$) is an N-terminally truncated and pyroglutamate-modified $A\beta$ peptide retaining highly hydrophobic, amyloidogenic, and neurotoxic properties. In Alzheimer's disease (AD) patients, $A\beta_{pE3-42}$ peptides accumulate into oligomers and induce cellular toxicity and synaptic dysfunction. $A\beta_{pE3-42}$ aggregates further seed the formation of amyloid plaques, which are the pathological hallmarks of AD. Given that $A\beta_{pE3-42}$ peptides play critical roles in the development of neurodegeneration, a reliable and reproducible synthetic access to these peptides may support pathological and medicinal studies of AD. Here, we synthesized $A\beta_{pE3-42}$ peptides through the microwave-assisted solid-phase peptide synthesis (SPPS). Utilizing thioflavin T fluorescence assay and dot blotting analysis with anti-amyloid oligomer antibody, the amyloidogenic activity of synthesized $A\beta_{pE3-42}$ peptides was confirmed. We further observed the cytotoxicity of $A\beta_{pE3-42}$ aggregates in cell viability test. To examine the cognitive deficits induced by synthetic $A\beta_{pE3-42}$ peptides, $A\beta_{pE3-42}$ oligomers were intracerebroventricularly injected into imprinting control region mice and Y-maze and Morris water maze tests were performed. We found that $A\beta_{pE3-42}$ aggregates altered the expression level of postsynaptic density protein 95 in cortical lysates. Collectively, we produced $A\beta_{pE3-42}$ peptides in the microwave-assisted SPPS and evaluated the amyloidogenic and pathological function of the synthesized peptides.

Alzheimer's disease (AD) is a progressive neurodegenerative disorder accompanied by amyloid plaques in the brain¹. The major components of plaques are amyloid- β ($A\beta$) peptides varying in length or N-/C-terminal modifications. One of the most abundant N-terminal truncated $A\beta$ variants is the pyroglutamate $A\beta_{3-42}$ ($A\beta_{pE3-42}$) peptide, which constitutes about a quarter of total $A\beta$ in the plaques^{2,3}. $A\beta_{pE3-42}$ is generated through a multistep protein modification starting from the sequential enzymatic cleavage of amyloid precursor protein to release $A\beta_{1-42}$ ⁴. Then, the two N-terminal amino acids, aspartic acid and alanine, of $A\beta_{1-42}$ are removed by amino peptidase A and dipeptidyl peptidase 4^{5,6}. Lastly, the truncated $A\beta_{3-42}$ peptide reacts with glutaminyl cyclase (QC), which converts the glutamate at the third position of N-terminus into a pyroglutamate⁷. The formation of a lactam ring from the pyroglutamate residue increases hydrophobicity, stability, and aggregation propensity of the $A\beta_{pE3-42}$ peptide compared to other $A\beta$ variants⁸. In AD brains, $A\beta_{pE3-42}$ peptides assemble into soluble oligomers inducing cognitive dysfunction and cellular toxicity^{9,10}. $A\beta_{pE3-42}$ oligomers are resistant to the degradation by peptidases and maintain stable β -sheet formation in the aqueous media¹¹. Insoluble $A\beta_{pE3-42}$ aggregates further accelerate the formation of plaques in AD patients¹². Recent clinical trials of an antibody drug candidate targeting $A\beta_{pE3-42}$ aggregates have provided the evidence that $A\beta_{pE3-42}$ is associated with amyloid plaques and cognitive impairments¹³. Thus, reproducible synthetic access to $A\beta_{pE3-42}$ peptide is essential for biochemical, neuropathological, and medicinal studies of AD. Unlike the full-length $A\beta$ isomers, $A\beta_{1-40}$ and $A\beta_{1-42}$, the production of

¹Department of Pharmacy, College of Pharmacy, Yonsei University, Incheon 21983, Republic of Korea. ²College of Pharmacy, Yonsei Institute of Pharmaceutical Sciences, Yonsei University, Incheon 21983, Republic of Korea. ³Department of Integrative Biotechnology and Translational Medicine, Yonsei University, Incheon 21983, Republic of Korea. ⁴Yonsei-POSTECH Campus, Pohang University of Science and Technology (POSTECH), Pohang, Gyeongbuk 37673, Republic of Korea. ✉email: hyeyunkim@yonsei.ac.kr; y.kim@yonsei.ac.kr

$A\beta_{pE3-42}$ peptides requires extra processes including removal of two N-terminal amino acids and cyclization of glutamate when acquired recombinantly¹⁴.

Here, we introduce a facile synthetic method of $A\beta_{pE3-42}$ production utilizing microwave-assisted solid-phase peptide synthesis (SPPS)¹⁵. To test aggregation propensity of the synthesized $A\beta_{pE3-42}$ peptides, we used in vitro assays, thioflavin T (ThT) assay and dot blotting analysis with anti-amyloid oligomer antibody. We tested the cellular toxicity of the synthesized $A\beta_{pE3-42}$ peptides in the cell viability assay. We then intracerebroventricularly injected $A\beta_{pE3-42}$ oligomers into imprinting control region (ICR) mouse models and performed behavior tests, Morris water maze and Y-maze tests, to identify cognitive deficits induced by synthesized $A\beta_{pE3-42}$ peptides. We further obtained brain lysates from the $A\beta_{pE3-42}$ -infused mouse models and analyzed the alteration of the synaptic protein marker levels by the western blot method.

Results and discussion

Synthesis of $A\beta_{pE3-42}$ peptides. Although $A\beta_{pE3-42}$ peptide is emerging as an attractive target for AD research, an effective synthetic method of this peptide is not yet developed. For the facile and reproducible production of $A\beta_{pE3-42}$, we utilized previously-reported $A\beta$ synthesis protocol using a microwave synthesizer for the preparation of $A\beta_{pE3-42}$ peptide¹⁶. Microwave-assisted SPPS improves the efficiency of the peptide synthesis due to reduce the reaction time and to suppresses the intermolecular aggregation, resulting in the inaccessibility of the coupling reagents to react with the peptide^{17,18}. Compared to the general approach of SPPS, microwave heating method increases the peptide yield from 20 to 70% and reduces the amino acid coupling time to 5 min (min)¹⁵. In microwave-assisted SPPS, we synthesized $A\beta_{pE3-42}$ peptide in 6.5 h (h) and obtained 71% peptide yield. This result showed that our synthetic approach minimizes the reaction time and enhances the peptide yield of $A\beta_{pE3-42}$. To conjugate the first C-terminal amino acids to the resin, we used the symmetric anhydride activation, and the following amino acids were sequentially synthesized to produce N-terminally truncated $A\beta_{4-42}$ peptides and additionally coupled pyroglutamates (Fig. 1). This approach brings in benefits to avoid complicated N-terminal cleavage and glutamate cyclization steps¹⁴. We further purified $A\beta_{pE3-42}$ peptides adapting reverse phase-high performance liquid chromatography analysis (Supplementary Fig. S1).

Aggregation properties of synthetic $A\beta_{pE3-42}$. During the progression of AD, $A\beta$ monomers aggregate into soluble oligomers and further become insoluble fibrils, the main components of the cerebral plaques in the brains¹⁹. As the misfolding and assembly is the key pathological feature of $A\beta$ in AD, it is critical to evaluate the aggregation properties of synthetically obtained peptides. Thus, to identify the aggregation propensity of the synthesized $A\beta_{pE3-42}$ peptide, we performed ThT fluorescence assay. ThT intercalates into the β -sheet formation of $A\beta$ fibrils, and the shifted fluorescence intensity of ThT upon β -sheet was measured to analyze the amounts of $A\beta$ fibrils²⁰. We prepared 25 μ M of $A\beta_{pE3-42}$ samples in deionized water with 5.5% dimethyl sulfoxide (DMSO) and incubated during the time range from 0 to 96 h at 37 °C. ThT solution (5 μ M) was added to each of incubated $A\beta$ solution samples and measured the intensity of ThT (Fig. 2a). We observed a saturation phase at 19 h of incubation, indicating the formation of β -sheet-rich $A\beta_{pE3-42}$ fibrils. We further compared the aggregation propensity of the synthesized $A\beta_{pE3-42}$ peptide with that of $A\beta_{1-42}$ and $A\beta_{4-42}$ peptides, which rapidly form aggregates²¹. Both of $A\beta_{1-42}$ and $A\beta_{4-42}$ peptides were produced through the previously reported synthesis protocol (Supplementary Fig. S2)¹⁶. In ThT assay, $A\beta_{pE3-42}$ formed β -sheet rich fibril after 19 h of incubation time, whereas $A\beta_{1-42}$ and $A\beta_{4-42}$ aggregated into fibrils after 23 and 28 h of incubation, respectively (Supplementary Fig. S3). This result was consistent with the previous report that N-terminal deletion or modification of $A\beta_{1-42}$ enhances the aggregation of N-terminal truncated $A\beta$ peptide compared to the $A\beta_{1-42}$ ²¹. As ThT assay is limited to detect β -sheet-rich fibrils,

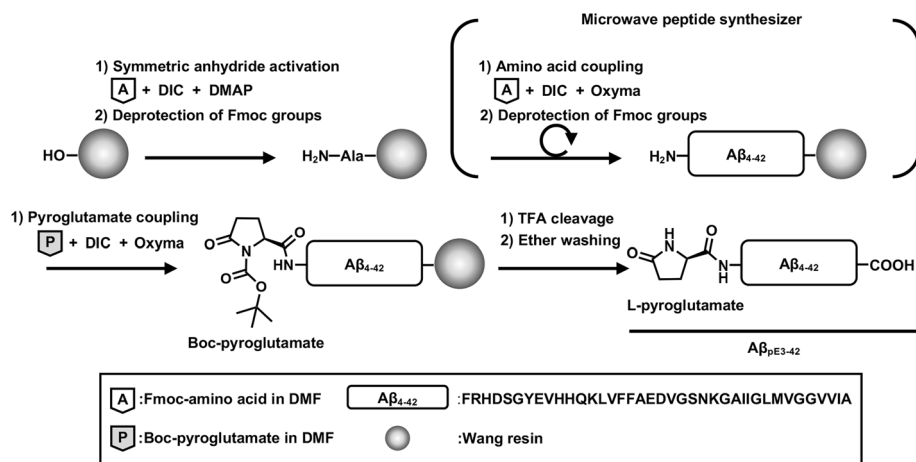


Figure 1. Scheme of $A\beta_{pE3-42}$ synthesis. A graphical scheme of $A\beta_{pE3-42}$ synthesis utilizing microwave-assisted SPPS. DMF, Dimethylformamide; $A\beta_{pE3-42}$, Pyroglutamate amyloid- β_{3-42} ; $A\beta_{4-42}$, Amyloid- β_{4-42} ; Boc, Tert-butoxycarbonylation; DIC, *N,N'*-diisopropylcarbodiimide; DMAP, 4-dimethylaminopyridine; Oxyma, Ethyl cyanohydroxyliminoacetate; TFA, Trifluoroacetic acid; Fmoc, 9-fluorenylmethyloxycarbonylation; Ala, Alanine.

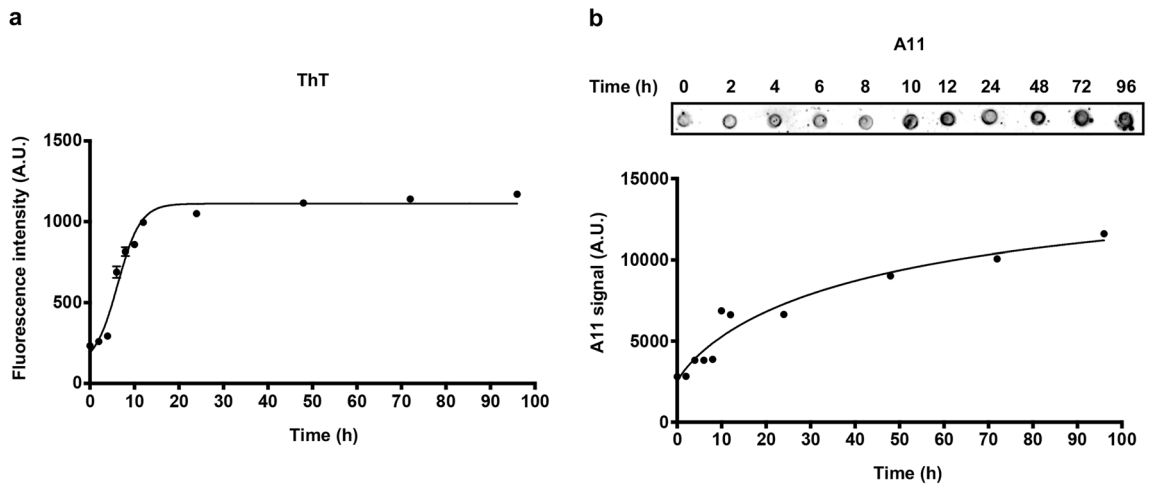


Figure 2. ThT fluorescence assay and dot blotting analysis of $A\beta_{pE3-42}$ aggregation. $A\beta_{pE3-42}$ (25 μ M) samples were incubated for the time points (0, 2, 4, 6, 8, 10, 12, 24, 48, 72, 96 h) at 37 °C. **(a)** Each of incubated $A\beta_{pE3-42}$ sample was interacted with ThT and the fluorescence intensity was measured by the fluorescence microplate reader. **(b)** Utilizing anti-oligomer polyclonal A11, dot blotting and densitometric analysis were performed to detect oligomeric forms of incubated $A\beta_{pE3-42}$ samples. The original dot blots and uncropped full-membrane results with A11 are presented in Supplementary Figure S4. The error bars represent S.E.M. $A\beta_{pE3-42}$, Pyroglutamate $A\beta_{3-42}$; h, Hours; A.U., Arbitrary units.

we performed dot blotting analysis using anti-amyloid oligomer A11 antibody for monitoring the formation of synthesized $A\beta_{pE3-42}$ oligomers²². We prepared 2 μ L of identical $A\beta_{pE3-42}$ samples used in ThT assay and loaded on the nitrocellulose membrane and performed dot blotting analysis (Fig. 2b). The levels of $A\beta_{pE3-42}$ oligomers were gradually increased until 96 h incubation. Interestingly, we observed oligomers even before the incubation at 37 °C (0 h incubation sample). This result supports the previous study that monomeric $A\beta_{pE3-42}$ sample has aggregates due to the spontaneous aggregation process of the peptide²³. Overall, we examined the amyloidogenic properties of the synthesized $A\beta_{pE3-42}$ peptides in both of ThT assay and dot blotting analysis.

Cell cytotoxicity induced by synthesized $A\beta_{pE3-42}$. To investigate the cellular toxicity of the synthesized $A\beta_{pE3-42}$ peptide, we treated $A\beta_{pE3-42}$ aggregates in HT22 cells (mouse hippocampal neuronal cell line). For the controls, we used $A\beta_{1-42}$ and $A\beta_{4-42}$ peptides, which induce cytotoxicity in neuronal cells²¹. To prepare the aggregated $A\beta$ variants ($A\beta_{1-42}$, $A\beta_{4-42}$, $A\beta_{pE3-42}$), each $A\beta$ variant (10 μ M) was incubated for 8 h at 37 °C. After seeding the cultured HT22 cells on a 96-well plate, we treated each incubated $A\beta$ variant for 24 h at 37 °C. We quantified the level of cell viability using 3-(4,5-dimethylthiazol-2-yl)-2,5-diphenyltetrazolium bromide (MTT) assay (Fig. 3)²⁴. Cell viability of $A\beta_{1-42}$, $A\beta_{4-42}$, and $A\beta_{pE3-42}$ groups were statistically compared to non-treated group (n = 3 per group). For the statistical analysis, we performed one-way ANOVA analysis followed by

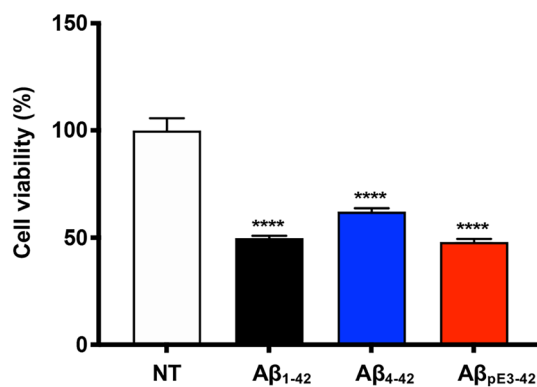


Figure 3. Cellular toxicity of synthesized $A\beta_{pE3-42}$ peptide. Synthesized $A\beta$ variants ($A\beta_{1-42}$, $A\beta_{4-42}$, $A\beta_{pE3-42}$) were prepared and each of aggregated $A\beta$ variant was treated in the cultured HT22 cell. After the treatment, the cell viability was measured utilizing MTT assay. Cell viability of $A\beta$ variants ($A\beta_{1-42}$, $A\beta_{4-42}$, $A\beta_{pE3-42}$) were statistically compared to non-treated group (4 groups, n = 3 per group). One-way ANOVA analysis followed by Bonferroni's *post-hoc* comparison tests were performed in all statistical analyses (**** $p < 0.0001$). The error bars represent S.E.M. NT, Non-treated; $A\beta_{1-42}$, Amyloid- β_{1-42} ; $A\beta_{4-42}$, Amyloid- β_{4-42} ; $A\beta_{pE3-42}$, Pyroglutamate amyloid- β_{3-42} .

Bonferroni's *post-hoc* comparison tests. Compared to the non-treated group, the cell viability was decreased to 48.1% ($p < 0.0001$) in $A\beta_{pE3-42}$ -treated group, 49.9% ($p < 0.0001$) in $A\beta_{1-42}$ -treated group, and 62.3% ($p < 0.0001$) in $A\beta_{4-42}$ -treated group. This result showed that all the $A\beta$ variants initiates cellular toxicity in the aggregated form. In cell viability assay, we confirmed that the synthetic $A\beta_{pE3-42}$ aggregates induce severe cellular toxicity in mouse hippocampal neuronal cells.

Cognitive impairments induced by synthetic $A\beta_{pE3-42}$ in rodents. To confirm the neuropathological function of the synthesized $A\beta_{pE3-42}$ peptide, we injected $A\beta_{pE3-42}$ oligomers into the lateral ventricular region of ICR mice as injected soluble $A\beta$ oligomers inducing neurotoxicity and cognitive decline²⁵. For comparison, we used $A\beta_{1-42}$ peptide, one of the major pathological forms of $A\beta$ variants associated with cognitive decline²⁶, as a control. $A\beta_{1-42}$ peptide was synthesized and purified through the previously reported protocol¹⁶. Since the dot blotting analysis result showed that soluble oligomers were clearly appeared after 8 h of incubation, we incubated 25 μ M of $A\beta$ solution for 8 h at 37 °C to prepare oligomeric samples for the injection. We conducted 5 μ L intracerebroventricular (ICV) injections of blank saline, $A\beta_{pE3-42}$ oligomer solution (10 μ M), and $A\beta_{1-42}$ oligomer solution (10 μ M) into brains of seven-week-old male ICR mice. After five days of recovery time, we performed learning and memory behavior tests, Y-maze and Morris water maze tests (Fig. 4a). All results from behavior tests were statistically compared to vehicle group ($n = 7$ per group). For the statistical analysis of the behavior tests, one-way ANOVA analysis followed by Bonferroni's *post-hoc* comparison tests were performed. Y-maze is widely applied to measure the short-term memory function of mouse models due to they normally explore new arm entries of the maze rather than the arm that was previously entered²⁷. We found that both of $A\beta_{pE3-42}$ ($p < 0.0001$) and $A\beta_{1-42}$ ($p < 0.001$) oligomers induced short-term memory impairments compared to

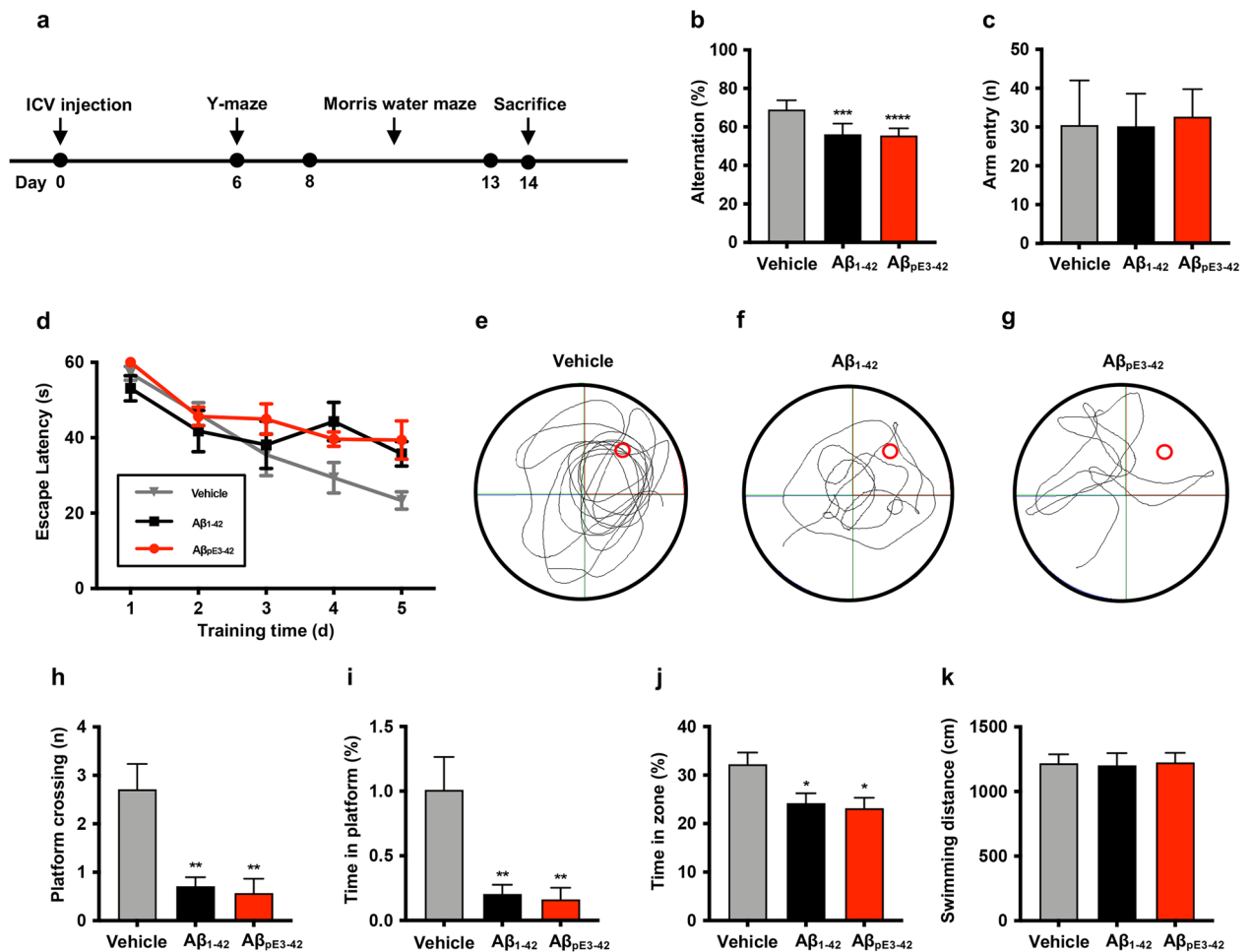


Figure 4. Y-maze and Morris water maze tests. (a) After 5 μ L ICV injection of saline, $A\beta_{pE3-42}$ (10 μ M, 10% DMSO in saline) and $A\beta_{1-42}$ (10 μ M, 10% DMSO in saline) into seven-week-old male ICR mice (3 groups, $n = 7$ per group), Y-maze and Morris water maze tests were performed. The data from Y-maze test indicated (b) the alteration percentages and (c) total arm entries of all groups. The results from Morris water maze test showed that (e–g) the representative motion tail, (h) crossing platform, (i) time in platform, time in target zone (j), and (k) total swimming distance of all groups. All data were statistically compared to vehicle group. One-way ANOVA analysis followed by Bonferroni's *post-hoc* comparison tests were performed in all statistical analyses ($*p < 0.05$, $**p < 0.01$, $***p < 0.001$, $****p < 0.0001$). The error bars represent S.E.M. $A\beta_{pE3-42}$, Pyroglutamate amyloid- β_{3-42} ; $A\beta_{1-42}$, Amyloid- β_{1-42} ; s, Seconds; d, Days.

vehicle (saline-injected) groups as the alternation levels were decreased (Fig. 4b). Total arm entry data showed that there were no significant differences of arm entries among all groups (Fig. 4c). After the Y-maze test, we performed Morris water maze test to examine the spatial learning dysfunction by $A\beta_{pE3-42}$ oligomers²⁸. During the five days of practice, we placed mice on four different quadrants in the water tank and measured time to reach the hidden platform for surviving in the water tank. In the trial day, we removed the platform and measured the crossing number, time in platform location, and time in zone. Compared to $A\beta_{pE3-42}$ and $A\beta_{1-42}$ groups, the escape latency of the vehicle groups was reduced on the fourth day of training (Fig. 4d). On the probe trial day, platform crossing number and time in platform of $A\beta_{pE3-42}$ ($p < 0.01$) and $A\beta_{1-42}$ groups ($p < 0.01$) were decreased comparing to the vehicle groups (Fig. 4e–i). We also analyzed the time in target quadrant and found that saline groups stay in the target quadrant longer than $A\beta_{pE3-42}$ ($p < 0.05$) and $A\beta_{1-42}$ groups ($p < 0.05$) (Fig. 4j). There were no significant differences of swimming distance among all groups (Fig. 4k). Overall, results from both of Y-maze and Morris water maze tests showed that the synthesized $A\beta_{pE3-42}$ aggregates induced impaired short-term and spatial memory function of mice.

Synaptic protein alteration by synthetic $A\beta_{pE3-42}$. As the behavior tests showed that synthesized $A\beta_{pE3-42}$ disrupted cognitive function of ICR mouse models, we sacrificed the ICV-injected mice and prepared brain lysates to further observe the changes of synaptic protein levels by $A\beta_{pE3-42}$ aggregates. Postsynaptic density protein 95 (PSD-95) regulates the synaptic strength of post-synaptic membrane, and synaptophysin supports synaptic vesicle endocytosis^{29,30}. Both of proteins are highly related to the synaptic plasticity and widely used biomarkers for cognitive function. In order to examine such alterations in synaptic plasticity, we used a western blot method to analyze PSD-95 and synaptophysin expression levels in the brain lysates of $A\beta_{pE3-42}$, $A\beta_{1-42}$, and saline groups (Fig. 5a). All the quantification of blots were statistically compared to vehicle group ($n = 4$ per group). For the statistical analysis of the quantification, one-way ANOVA analysis followed by Bonferroni's *post-hoc* comparison tests were performed. PSD-95 expression levels were decreased within the cortex region of $A\beta_{pE3-42}$ ($p < 0.0001$) and $A\beta_{1-42}$ groups ($p < 0.001$) compared to the saline groups (Fig. 5b). However, there was no change of synaptophysin levels among three groups (Fig. 5c). In the hippocampus region, both PSD-95 and synaptophysin expression levels were not significantly altered in $A\beta_{pE3-42}$ and $A\beta_{1-42}$ groups (Fig. 5d,e). All results from the western blot assay showed that the synthesized $A\beta_{1-42}$ and $A\beta_{pE3-42}$ oligomers suppress postsynaptic memory function in cortical region of the mice.

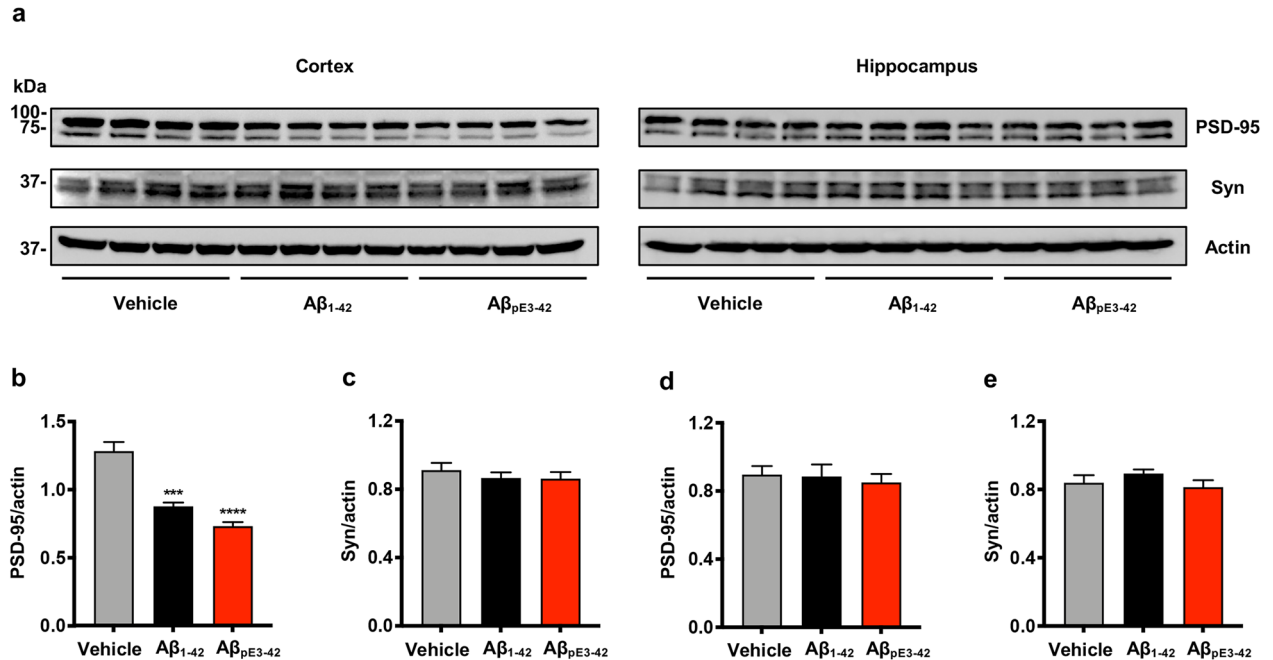


Figure 5. $A\beta_{pE3-42}$ -induced down-regulation of postsynaptic protein level in cortical lysate. (a) Western blot analysis of PSD-95 (85 kDa), synaptophysin (40 kDa), and β -actin (38 kDa) expression in hippocampal and cortical lysates of vehicles, $A\beta_{1-42}$ -infused mouse models, and $A\beta_{pE3-42}$ -infused mouse models. The original and uncropped full-membrane results with PSD-95, synaptophysin, and actin are presented in Supplementary Figure S5. Densitometry of PSD-95 and synaptophysin in (b,c) cortical and (d,e) hippocampal region. The intensities of blots were normalized to actin and statistically compared to vehicle (3 groups, $n = 4$ per group). One-way ANOVA analysis followed by Bonferroni's *post-hoc* comparison tests were performed in all statistical analyses (** $p < 0.001$, **** $p < 0.0001$). The error bars represent S.E.M. PSD-95, Postsynaptic density protein 95; Syn, Synaptophysin; Actin, β -actin; $A\beta_{pE3-42}$, Pyroglutamate amyloid- β_{3-42} ; $A\beta_{1-42}$, Amyloid- β_{1-42} , kDa, Kilodaltons.

Conclusion

In this study, we investigated a facile synthetic method of $A\beta_{pE3-42}$ peptides and confirmed the amyloidogenic and pathologic properties of the synthesized peptides. In ThT assay and dot blotting analysis, we found that $A\beta_{pE3-42}$ peptides rapidly accumulate into oligomers and fibrils. We further examined cytotoxicity of synthetic $A\beta_{pE3-42}$ aggregates. Utilizing $A\beta_{pE3-42}$ -infused mouse models, we performed Y-maze and Morris water maze tests and observed synaptic dysfunction induced by synthetic $A\beta_{pE3-42}$ oligomers. Furthermore, the expression level of PSD-95 was decreased in the cortical region of $A\beta_{pE3-42}$ -infusion mouse models compared to the vehicle groups. As $A\beta_{pE3-42}$ aggregates are highly associated with AD, the presented synthetic method of $A\beta_{pE3-42}$ will support pathological, therapeutic, and diagnostic investigation of the disorder.

Methods

Materials. Fmoc-Ala-OH, Fmoc-Arg(pbf)-OH, Fmoc-Asn(trt)-OH, Fmoc-Asp(OtBu)-OH, Fmoc-Cys(trt)-OH, Fmoc-Gln(trt)-OH, Fmoc-Glu(OtBu)-OH, Fmoc-Gly-OH, Fmoc-His(trt)-OH, Fmoc-Ile-OH, Fmoc-Leu-OH, Fmoc-Lys(Boc)-OH, Fmoc-Met-OH, Fmoc-Phe-OH, Fmoc-Ser(tBu)-OH, Fmoc-Tyr(tBu)-OH, and Fmoc-Val-OH were purchased from CEM (USA). Wang resin LS (0.22 mmol/g) was purchased from Advanced ChemTech (USA). Trifluoroacetic acid (TFA), triisopropylsilane, and 3,6-dioxa-1,8-octanedithiol (DODT), were purchased from TCI (Japan). Dimethylformamide (DMF), dichloromethane (DCM), and dimethyl sulfoxide (DMSO) were purchased from SAMCHUN chemical (Korea). Ether and acetonitrile were purchased from J.T Baker (USA). *N,N'*-diisopropylcarbodiimide (DIC), 4-dimethylaminopyridine (DMAP), ethyl cyanohydroxylaminoacetate (Oxyma), piperidine, Boc-Pyr-OH, and ThT were purchased from sigma Sigma-Aldrich (USA). 96-well half area black plate was purchased from Corning (USA). 1X protease inhibitor cocktail was purchased from Roche Diagnostics (Switzerland). Pierce BCA protein assay kit was purchased from Thermo Fisher Scientific (USA).

Animal preparation. Seven-week-old male ICR mice were purchased from Orient Bio Inc (Republic of Korea) and habituated for five days before the ICV injection. After the injection, behavior tests were performed.

Ethical approval. All animal experiments were carried out in accordance with the National Institutes of Health (NIH) guide for the care, the use of laboratory animals (NIH Publications), and the ARRIVE guidelines. The research protocols were authorized by the Institutional Animal Care and Committee of Yonsei University (Seoul, Republic of Korea, IACUC-202103–1221-01).

Safety statement. TFA is an acid, which severely irritates and burns the skin and eyes. Furthermore, breathing TFA will damage nose and throat. Thus, the protective clothes, goggles, and gloves are required before treating TFA.

Synthesis of $A\beta_{pE3-42}$ peptides. $A\beta_{4-42}$ peptide was synthesized through the previous Fmoc SPPS protocol¹⁶. For the first C-terminal alanine coupling, symmetric anhydride activation was utilized. We dissolved 1 mmol of DIC, 51 mg of 4-dimethylaminopyridine, and 2.2 mmol of Fmoc-Ala-OH dissolved in 2 mL of DMF/DCM (1:1 v/v) solution. In the solid-phase synthesis cartridge, DMF swelled Wang resin LS and the mixture were added and placed on a shaker for 1 h. After the complete symmetric anhydride activation, the rest of the amino acids were coupled by automated peptide synthesized (Liberty Blue, CEM, USA) with coupling reagents (1.0 M Oxyma pure and 1.0 M DIC solution in DMF) and deprotecting reagent (20% piperidine solution in DMF). After the synthesis of the truncated $A\beta_{4-42}$ peptide, 1.1 mmol of Boc-Pyr-OH solution in DMF and coupling reagents (1.0 M Oxyma and 1.0 M DIC solution in DMF) were added to $A\beta_{4-42}$ peptide on solid supports and reacted for 4 h. After the complete synthesis of $A\beta_{pE3-42}$ peptide, 92.5% TFA cocktail (92.5:2.5:2.5:2.5 TFA/deionized water/triisopropylsilane/DODT, v/v/v/v) solution was added to the peptide bound resins and reacted for 4 h to cleave side chain protecting groups and Wang resin LS from the peptides. After cleavage of the peptides, we evaporated TFA solution by a rotary evaporator and added cold anhydrous ether (stored in -20°C) to yield the crude peptides. The peptides were isolated from the ether solution by centrifugation (3000 rpm, 15 min). The isolated mass and percent yield were 0.306 g and 71%, respectively.

Purification of $A\beta_{pE3-42}$ peptides. To purify and analyze the synthesized $A\beta_{pE3-42}$ peptides, RP-HPLC was used with binary gradients of solvents A (0.1% TFA in deionized water) and B (0.09% TFA in acetonitrile). We utilized 5 μm biphenyl 250 \times 21.2 mm column (Phenomenex, USA) with binary gradients from 20 to 55% of solvent B (6 mL/min, 38 min) and 5 μm biphenyl 250 \times 4.6 mm column (Phenomenex, USA) with binary gradients from 10 to 90% of solvent B (0.8 mL/min, 38 min) for the purification and analysis of the peptides. The UV detection of all the peptides were conducted at 230 nm.

Preparation of $A\beta_{1-42}$ and $A\beta_{4-42}$ peptides. To compare the amyloidogenic and neuropathological effects of $A\beta_{pE3-42}$ peptide, $A\beta_{1-42}$ and $A\beta_{4-42}$ peptide were used as a control. $A\beta_{1-42}$ and $A\beta_{4-42}$ peptides were synthesized and purified utilizing the previously reported $A\beta$ synthesis protocol¹⁶.

ThT fluorescence assay. To monitor the aggregation propensity and quantify the β -sheet formation in $A\beta_{pE3-42}$ aggregates, ThT fluorescence assay was performed. $A\beta_{pE3-42}$ peptide was dissolved in DMSO (1 mM) and diluted with deionized water to make $A\beta_{pE3-42}$ solution (25 μM). Each of sample was incubated for the various time range (1, 2, 4, 6, 8, 12, 24, 48, 72, 96 h) at 37°C . After the incubation, 25 μL of the incubated $A\beta_{pE3-42}$ samples

and 75 μL of ThT solution (5 μM ThT in 50 mM glycine buffer, pH 8.9) were added in a 96-well half area black plate. Fluorescence intensity of ThT ($\lambda_{\text{ex}} = 450 \text{ nm}/\lambda_{\text{em}} = 485 \text{ nm}$) intercalated within $\text{A}\beta_{\text{pE3-42}}$ aggregates was measured by using the microplate reader. To compare the aggregation propensities of $\text{A}\beta_{4-42}$, $\text{A}\beta_{1-42}$, and $\text{A}\beta_{\text{pE3-42}}$, ThT assay was performed under the identical conditions as described above.

Dot blotting analysis. To identify $\text{A}\beta_{\text{pE3-42}}$ oligomers, each of $\text{A}\beta_{\text{pE3-42}}$ samples (25 μM) was incubated for the time range (0, 2, 4, 6, 8, 12, 24, 48, 72, 96 h) at 37 °C. 2 μL of each $\text{A}\beta_{\text{pE3-42}}$ sample was loaded on a nitrocellulose membrane and blocked with a 5% skim milk solution for 1 h. After the blocking, we washed the membrane with TBST (tris-buffered saline with 0.1% Tween 20) for three times and incubated with primary antibody A11 (1:2000, Invitrogen, USA) for overnight at 4 °C. After removing the primary antibody and washing the membrane with TBST for three times and added HRP-conjugated goat anti-rabbit secondary antibody (1:10,000, Bethyl Laboratories, USA) and incubated for 1 h at room temperature. Membranes were washed three times with TBST, and the proteins on the membranes were developed using ECL kit (Thermo Fisher Scientific, USA).

Cell viability assays. HT 22 cell was purchased from the Korean Cell line Bank (Seoul National University, Republic of South Korea) and cultured in the Dulbecco's Modified Eagle's medium (DMEM) (Thermo Fisher Scientific, USA) with 10% foetal bovine serum and 1% penicillin. The cytotoxic effect of synthesized $\text{A}\beta_{1-42}$, $\text{A}\beta_{4-42}$, and $\text{A}\beta_{\text{pE3-42}}$ was investigated using the previously reported MTT assay protocol²⁴. Cultured HT22 cell (8×10^3 cells/well) was seeded on a 96-well plate. Each $\text{A}\beta$ variant (10 μM) was prepared in starvation medium (0.5% foetal bovine serum and 1% penicillin in DMEM) and treated on the plate for 24 h at 37 °C. 15 μL of MTT reagent (Promega, USA) was added to each well and incubated for additional 4 h at 37 °C. Finally, 100 μL of solubilization solution (Promega, USA) was added for 30 min at 37 °C. The absorbance was measured at 570 nm.

ICV injection. To examine cognitive deficits induced by $\text{A}\beta_{\text{pE3-42}}$ oligomers, $\text{A}\beta_{\text{pE3-42}}$ (10 μM in saline) was incubated for 6 h and 5 μL of $\text{A}\beta_{\text{pE3-42}}$ oligomers were intracerebroventricularly injected to ICR mouse using the previously reported ICV injection protocol²⁵.

Y-maze. For observing the short-term memory dysfunction initiated by $\text{A}\beta_{\text{pE3-42}}$ oligomers, Y-maze test was performed. The maze was built with three arm entries (40 cm long, 10 cm wide, 12 cm high), which were symmetrically disposed at 120° angles. Each of mouse was placed at the edge of the arm entry and allowed to move around the maze for 8 min. After recording the experiment, the number of total arm entries and sequence of arm choices were analyzed. The percent alternation was calculated by the proportion of arm choices that differ from the previous two choices. After the trial, the maze was cleaned with 70% ethanol solution before the next trials.

Morris water maze. Morris water maze tests were performed to monitor deficits of spatial learning function induced by $\text{A}\beta_{\text{pE3-42}}$ oligomers. The maze contained a circular water tank (120 cm diameter, 25 ± 1 °C) with the hidden quadrant, which was placed 1.5 cm below the water surface. The maze is equally divided into four quadrants (A,B,C,D) and three different shapes of cues are located on the top of quadrant B, C, and D to provide the direction for the mice. The hidden platform is placed on the middle of quadrant C and mice can survive if they reach the platform. The tank is filled with water with non-toxic white paint to prevent the chances that mice can see the hidden platform. We performed five days of training with four trials per day. In each trial, mouse was placed at the end of quadrant and allowed to swim and reach the platform for 60 s. After 60 s of trial, we took the mouse out of the maze and provided 10 min of resting time before the next trial. We measured escape latency, which is the average of the time to reach the platform during four trials. On the sixth day, we performed 60 s of probe test. Each mouse was placed at the edge of the opposite quadrant of the target zone. The hidden platform was removed and we analyzed crossing number, time in platform, time in the target quadrant, and swimming distance.

Lysate preparation. After the behavior tests, we sacrificed all the mice to prepare brain lysates. We dissected the hippocampal and cortical regions of brains. All the brain lysates were homogenized in ice-cold RIPA buffer with 1X protease inhibitor cocktail. Homogenized brain lysates were incubated in ice for 20 min and collected the supernatants after the centrifugation at 14 000 rpm at °C for 30 min. The protein concentrations in supernatants were quantified via Pierce BCA protein assay kit.

Western blot. To analyze the alternation of synaptic protein marker levels, PSD-95 and synaptophysin levels, by $\text{A}\beta_{\text{pE3-42}}$ aggregates, we conducted the western blot analysis. For the experiment, 15 μg of cortical and hippocampal brain lysates were loaded on the 12% gel and separated by sodium dodecyl sulfate polyacrylamide gel electrophoresis. We transferred the proteins from the gel to a nitrocellulose membrane and the membranes were blocked with a 5% skim milk solution for 1 h. After the blocking, we washed the membrane with TBST (tris-buffered saline with 0.1% Tween 20) for three times and incubated with primary antibody PSD-95 (1:2000, Invitrogen, USA) or synaptophysin (1:1000, MilliporeSigma, USA) for overnight at 4 °C. After removing the primary antibody and washing the membrane with TBST for three times and added HRP-conjugated goat anti-mouse secondary antibody (1:10000, Bethyl Laboratories, USA) and incubated for 2 h at room temperature. Membranes were washed three times with TBST, and the proteins on the membranes were developed using ECL kit (Thermo Fisher Scientific, USA). For control of the protein loading levels, we used β -actin (1:2000, MilliporeSigma, USA).

Statistical analysis. All graphical data were analyzed through GraphPad Prism 9.0 software, and statistical analyses were obtained from the one-way ANOVA followed by Bonferroni's posthoc comparisons. The error bars represent the standard error of the mean (S.E.M).

Equipment and settings. The scheme of A β _{pE3-42} synthesis was drawn by power point 16.56. Prism 9.0 was used to statistically analyze and visualize ThT fluorescence assay, cell viability assay, and behavior test results. FUSION Solo S and Image J Fiji 1.0. were used to visualize, quantify, and acquire dot blotting of A β _{pE3-42} aggregates with A11 and western blot of hippocampal and cortical lysates of A β _{pE3-42}-infused mouse models, A β ₁₋₄₂-infused mouse models, and vehicles. All the quantification data were organized into graphical data with Prism 9.0.

Data availability

All data generated or analyzed during this study are included in this published article (and its Supplementary Information files).

Received: 22 August 2022; Accepted: 16 December 2022

Published online: 10 January 2023

References

- DeTure, M. A. & Dickson, D. W. The neuropathological diagnosis of Alzheimer's disease. *Mol. Neurodegener.* **14**, 32 (2019).
- Wildburger, N. C. *et al.* Diversity of amyloid-beta proteoforms in the Alzheimer's disease brain. *Sci. Rep.* **7**, 9520 (2017).
- Portelius, E. *et al.* Mass spectrometric characterization of brain amyloid beta isoform signatures in familial and sporadic Alzheimer's disease. *Acta. Neuropathol.* **120**, 185–193 (2010).
- Hariyaya, Y. *et al.* Amyloid β protein starting pyroglutamate at position 3 is a major component of the amyloid deposits in the Alzheimer's disease brain. *Biochem. Biophys. Res. Commun.* **276**, 422–427 (2000).
- Sevally, J. *et al.* Aminopeptidase A contributes to the N-terminal truncation of amyloid beta-peptide. *J. Neurochem.* **109**, 248–256 (2009).
- Antonyan, A. *et al.* Concerted action of dipeptidyl peptidase IV and glutaminyl cyclase results in formation of pyroglutamate-modified amyloid peptides in vitro. *Neurochem. Int.* **113**, 112–119 (2018).
- Schilling, S. *et al.* Glutaminyl cyclase inhibition attenuates pyroglutamate A β and Alzheimer's disease-like pathology. *Nat. Med.* **14**, 1106–1111 (2008).
- Jawhar, S., Wirths, O. & Bayer, T. A. Pyroglutamate amyloid- β (A β): A hatchet man in Alzheimer disease. *J. Biol. Chem.* **286**, 38825–38832 (2011).
- Grochowska, K. M. *et al.* Posttranslational modification impact on the mechanism by which amyloid- β induces synaptic dysfunction. *EMBO. Rep.* **18**, 962–981 (2017).
- Youssef, I. *et al.* N-truncated amyloid-beta oligomers induce learning impairment and neuronal apoptosis. *Neurobiol. Aging.* **29**, 1319–1333 (2008).
- Bayer, T. A. Pyroglutamate A β cascade as drug target in Alzheimer's disease. *Mol. Psychiatry.* **1**, 1880–1885 (2021).
- Dammers, C., Schwarten, M., Buell, A. K. & Willbold, D. Pyroglutamate-modified A β (3–42) affects aggregation kinetics of A β (1–42) by accelerating primary and secondary pathways. *Chem. Sci.* **8**, 4996–5004 (2017).
- Espay, A. J. Donanemab in early Alzheimer's disease. *N. Engl. J. Med.* **385**, 666–667 (2021).
- Dammers, C. *et al.* Purification and characterization of recombinant N-terminally pyroglutamate-modified amyloid- β variants and structural analysis by solution NMR spectroscopy. *PLoS ONE* **10**, e0139710 (2015).
- Pedersen, S. L., Tofteng, A. P., Malik, L. & Jensen, K. J. Microwave heating in solid-phase peptide synthesis. *Chem. Soc. Rev.* **41**, 1826–1844 (2012).
- Choi, J. W., Kim, H. Y., Jeon, M., Kim, D. J. & Kim, Y. Efficient access to highly pure β -amyloid peptide by optimized solid-phase synthesis. *Amyloid* **19**, 133–137 (2012).
- Marek, P., Woys, A. M., Sutton, K., Zanni, M. T. & Raleigh, D. P. Efficient microwave-assisted synthesis of human islet amyloid polypeptide designed to facilitate the specific incorporation of labeled amino acids. *Org. Lett.* **12**, 4848–4851 (2010).
- Masuda, K. *et al.* Microwave-assisted solid-phase peptide synthesis of neurosecretory protein GL composed of 80 amino acid residues. *J. Pept. Sci.* **21**, 454–460 (2015).
- Chen, G. F. *et al.* Amyloid beta: Structure, biology and structure-based therapeutic development. *Acta. Pharmacol. Sin.* **38**, 1205–1235 (2017).
- Sebastiao, M., Quittot, N. & Bourgault, S. Thioflavin T fluorescence to analyse amyloid formation kinetics: Measurement frequency as a factor explaining irreproducibility. *Anal. Biochem.* **532**, 83–86 (2017).
- Bouter, Y. *et al.* N-truncated amyloid β (A β) 4–42 forms stable aggregates and induces acute and long-lasting behavioral deficits. *Acta. Neuropathol.* **126**, 189–205 (2013).
- Pryor, N. E., Moss, M. A. & Hestekin, C. N. Unraveling the early events of amyloid- β protein (A β) aggregation: Techniques for the determination of A β aggregate size. *Int. J. Mol. Sci.* **13**, 3038–3072 (2012).
- Festa, G. *et al.* Aggregation states of A β ₁₋₄₀, A β ₁₋₄₂ and A β _{p3-42} amyloid beta peptides: A SANS Study. *Int. J. Mol. Sci.* **20**, 4126 (2019).
- Yang, S. H. *et al.* Nec-1 alleviates cognitive impairment with reduction of A β and tau abnormalities in APP/PS1 mice. *EMBO. Mol. Med.* **9**, 61–77 (2017).
- Kim, H. Y., Lee, D. K., Chung, B. R., Kim, H. V. & Kim, Y. Intracerebroventricular injection of amyloid- β peptides in normal mice to acutely induce Alzheimer-like cognitive deficits. *J. Vis. Exp.* **109**, 53309 (2016).
- Yeung, J. H. Y. *et al.* The acute effects of amyloid-beta₁₋₄₂ on glutamatergic receptor and transporter expression in the mouse hippocampus. *Front. Neurosci.* **13**, 1427 (2019).
- Kraeuter, A. K., Guest, P. C. & Sarnyai, Z. The Y-maze for assessment of spatial working and reference memory in mice. *Methods. Mol. Biol.* **1916**, 105–111 (2019).
- Vorhees, C. V. & Williams, M. T. Morris water maze: Procedures for assessing spatial and related forms of learning and memory. *Nat. Protoc.* **1**, 848–858 (2006).
- El-Husseini Ael, D. *et al.* Synaptic strength regulated by palmitate cycling on PSD-95. *Cell* **108**, 849–863 (2022).
- Wiedenmann, B., Franke, W. W., Kuhn, C., Moll, R. & Gould, V. E. Synaptophysin: A marker protein for neuroendocrine cells and neoplasms. *Proc. Natl. Acad. Sci. USA* **83**, 3500–3504 (1986).

Acknowledgements

This research was supported by the Korea Health Technology R&D Project (Grant Number: HU21C0161, YK) through the Korea Health Industry Development Institute (KHIDI) and Korea Dementia Research Center (KDRC), and Mid-Career Researcher Program (Grant Number: NRF-2021R1A2C2093916, YK; NRF-2021R1A2C1013247, HK), and Basic Science Research Program (Grant Number: NRF-2018R1A6A1A03023718, YK and HK) through the National Research Foundation of Korea (NRF), funded by the Ministry of Health & Welfare and Ministry of Science and ICT, Republic of Korea. This research was also supported by Amyloid Solution and POSCO Science Fellowship of POSCO TJ Park Foundation.

Author contributions

I.C. led and performed all experiments. H.L. intracerebroventricularly injected $A\beta_{pE3-42}$ and $A\beta_{1-42}$ peptides to ICR mouse. D.L. prepared and habituated ICR mouse. I.W.P. and S.Y. synthesized and purified $A\beta_{1-42}$ peptides. I.C., H.Y.K., and Y.K. contributed to the manuscript preparation. H.Y.K. and Y.K. supervised the project.

Competing interests

Y.K. is an employee to Amyloid Solution, received equity or equity options. The rest of other authors do not have any conflict of interest.

Additional information

Supplementary Information The online version contains supplementary material available at <https://doi.org/10.1038/s41598-022-26616-x>.

Correspondence and requests for materials should be addressed to H.Y.K. or Y.K.

Reprints and permissions information is available at www.nature.com/reprints.

Publisher's note Springer Nature remains neutral with regard to jurisdictional claims in published maps and institutional affiliations.



Open Access This article is licensed under a Creative Commons Attribution 4.0 International License, which permits use, sharing, adaptation, distribution and reproduction in any medium or format, as long as you give appropriate credit to the original author(s) and the source, provide a link to the Creative Commons licence, and indicate if changes were made. The images or other third party material in this article are included in the article's Creative Commons licence, unless indicated otherwise in a credit line to the material. If material is not included in the article's Creative Commons licence and your intended use is not permitted by statutory regulation or exceeds the permitted use, you will need to obtain permission directly from the copyright holder. To view a copy of this licence, visit <http://creativecommons.org/licenses/by/4.0/>.

© The Author(s) 2023